

This is an Open Access document downloaded from ORCA, Cardiff University's institutional repository:<https://orca.cardiff.ac.uk/id/eprint/109107/>

This is the author's version of a work that was submitted to / accepted for publication.

Citation for final published version:

Hussain, Mudassar, Misbah-ul-Islam, Misbah-ul-Islam, Meydan, Turgut , Cuenca, Jerome A. , Melikhov, Yevgen , Mustafa, Ghulam, Murtaza, Ghulam and Jamil, Yasir 2018. Microwave absorption properties of CoGd substituted ZnFe₂O₄ ferrites synthesized by co-precipitation technique. *Ceramics International* 44 (6) , pp. 5909-5914. 10.1016/j.ceramint.2017.12.145

Publishers page: <http://dx.doi.org/10.1016/j.ceramint.2017.12.145>

Please note:

Changes made as a result of publishing processes such as copy-editing, formatting and page numbers may not be reflected in this version. For the definitive version of this publication, please refer to the published source. You are advised to consult the publisher's version if you wish to cite this paper.

This version is being made available in accordance with publisher policies. See <http://orca.cf.ac.uk/policies.html> for usage policies. Copyright and moral rights for publications made available in ORCA are retained by the copyright holders.



Microwave Absorption Properties of CoGd Substituted ZnFe₂O₄ Ferrites Synthesized by Co-precipitation Technique

Mudassar Hussain^{a,b}, Misbah-ul-Islam^a, Turgut Meydan^{b*}, Cuenca J.A.^b,
Yevgen Melikhov^b, Ghulam Mustafa^a, Ghulam Murtaza^a, Yasir Jamil^c

^a Department of Physics, Bahauddin Zakariya University, Multan 60800, Pakistan

^b Wolfson Centre for Magnetism, School of Engineering, Cardiff University, Cardiff, CF24 3AA, United Kingdom

^c Department of Physics, University of Agriculture, Faisalabad 38040, Pakistan

Abstract

A series of co-precipitated Zn_{1-x}Co_xGd_yFe_{2-y}O₄ spinel ferrites (x=0.0-0.5, y=0.00-0.10) sintered at 1000°C were characterized by X-ray diffraction (XRD), Fourier transform infrared spectroscopy (FTIR), scanning electron microscopy (SEM), vibrating sample magnetometry (VSM) and microwave cavity perturbation (MCP). XRD patterns and FTIR spectra reveal formation of the spinel phase along with few traces of GdFeO₃ second phase. The lattice constant decreases with an increasing amount of CoGd ions due to the segregation of Gd³⁺ on the grain boundaries and due to replacement of larger Zn²⁺ ions with smaller Co²⁺ ions. SEM shows grain size to decrease with the increase of CoGd contents due to grain growth inhibition by the second phase. VSM results show remanence and saturation magnetization to exhibit an increasing trend due to Co substitution on octahedral sites and presence of a second phase. The coercivity increases with the increase of CoGd contents due to anisotropic nature of Co. MCP shows the complex magnetic permeability to increase with CoGd concentration while the complex permittivity decreases.

Keywords:

Spinel ferrites, magnetization, permittivity, permeability

*Corresponding author: Email meydan@cardiff.ac.uk (Dr.Turgut Meydan)

1. Introduction

In the past few years, with the rapid advancement of wireless communication, electromagnetic interference (EMI) has become a prevalent issue in the design of electronic devices. In order to mitigate the effects of EMI, new materials with good microwave absorption properties (described by the microwave permittivity and permeability) are required. Spinel ferrites are among the materials that potentially could be widely utilized in the frequency range from C-band to X-band. As reported earlier, the properties of ferrites can be tailored using appropriate dopant for different applications [1-8]. Many researchers have reported the complex permittivity and permeability of spinel ferrites that are doped with different elements, to achieve a better choice of microwave absorption for different applications ,e.g. stealth technology or the shielding of the circuits of medical devices from microwaves (Bluetooth and Wi-Fi, etc.) [9-13]. Spinel ferrites can be synthesized by various methods; amongst the most common being co-precipitation, hydrothermal, combustion, micro-emulsion, polymer-pyrolysis and sol-gel [14-19]. The co-precipitation technique offers several advantages over the others including processing at low temperature and/or better homogeneity, fine particle size etc. Co-substitution can also be easily achieved by the co-precipitation technique, which eventually could lead to the enhancement of the microwave absorption properties of the base ferrites. It was reported that microwave properties can be tuned by doping the spinel ferrites with metallic ions Ni, Co, Zn [11] and similarly that rare earth (RE) elements like Gadolinium can affect the magnetic and dielectric properties of the material [20-22]. In this study, CoGd substituted Zn-ferrites ($Zn_{1-x}Co_xGd_yFe_{2-y}O_4$) samples are prepared by the co-precipitation technique, with the overall aim of improving the magnetic parameters necessary for microwave absorbers and other potential applications at high frequencies.

2. Materials and Methods

2.1. Sample Preparation

Spinel ferrites with general formula $Zn_{1-x}Co_xGd_yFe_{2-y}O_4$ ($x=0.0-0.5$, $y=0.00-0.10$) were prepared by the co-precipitation technique with the following analytical grade reagents: $CoCl_2 \cdot 6H_2O$, $Zn(NO_3)_2 \cdot 6H_2O$, $Gd(NO_3)_3 \cdot 6H_2O$ and $Fe(NO_3)_3 \cdot 9H_2O$. The precursor materials were dissolved in de-ionized water in the desired stoichiometric proportions using an ultrasonic cleaner and subsequently stirred using a magnetic stirrer on a hot plate at 60°C. The pH of the solution was adjusted, in the range pH 10 to pH 11 using ammonia solution. The beaker containing the

precipitates along with the solution was kept in a preheated water bath at 80°C for 90 minutes under the ambient atmosphere. The precipitates were filtered, washed several times with deionized water to remove impurities and dried at 100°C for 12 hours in an oven at 100°C. The dried powder was ground in an agate mortar and pestle to obtain fine powder. The fine powder was pelletized under a pressure of 30kN. Finally, the ferrite powder and the pellets were sintered at 1000°C for 6 hours in a muffle furnace.

2.2. Characterization of the samples

The Fourier transform infrared spectroscopy (FTIR) spectra were recorded in the wave number range 400–4000 cm^{-1} using Perkin Elmer spectrometer. The x-ray diffraction (XRD) patterns of the powdered samples were obtained at room temperature using a Philips Xpert PANalytical diffractometer operating at 30 mA and 40 kV. The surface morphology and elemental investigation was performed using a JSM-6490 JEOL Scanning Electron Microscope (SEM) equipped with energy-dispersive x-ray (EDX) spectroscopy. The Magnetization Hysteresis loops were recorded at room temperature using a Vibrating Sample Magnetometer (VSM, model Lake Shore 735). The complex permittivity and permeability in the frequency range 2.5 to 6.8 GHz and 3.8 to 10.16 GHz respectively were achieved using microwave cavity perturbation (MCP) on an Agilent (Keysight) N5232APNA-L microwave Vector Network Analyzer with a cylindrical cavity resonator. The cavity was placed in a Memmert IPP 400 oven at 25°C. First, an empty quartz tube without sample was placed in the cavity and then the tube loaded with sample was placed in the cavity. The results were collected using software designed in NI LabVIEW using cavity perturbation theory [23-25]. The following equations were used to calculate the permittivity and permeability, while another formula was also used to calculate permeability in a demagnetizing field orientation details of which has been published earlier [23-25]:

$$\epsilon_{\text{eff}}' = -2 \frac{(\Delta f)}{f_o} \frac{V_c}{V_s} G_{mnp} + 1 \quad (1)$$

$$\epsilon_{\text{eff}}'' = \frac{(\Delta BW)}{f_o} \frac{V_c}{V_s} G_{mnp} \quad (2)$$

$$\mu_{\text{eff}}' = 2 \frac{(\Delta f)}{f_o} \frac{V_c}{V_s} G_{mnp} + 1 \quad (3)$$

$$\mu_{\text{eff}}'' = \frac{(\Delta BW)}{f_o} \frac{V_c}{V_s} G_{mnp} \quad (4)$$

where ϵ_{eff}' and ϵ_{eff}'' are real part and imaginary part of complex permittivity; μ_{eff}' and μ_{eff}'' are the real and imaginary part of complex permeability, respectively; Δf and ΔBW are the change in resonant frequency and bandwidth, respectively; V_S and V_C are sample volume and cavity volume, respectively; G_{mnp} is the mode dependent field scaling constant. Effective values are quoted for a powder sample and accounts for any finite air spaces between the particles. The calculated values are thus quoted as “effective” which are smaller than their intrinsic values.

3. Results and Discussion

3.1. FTIR Spectra

FTIR spectra recorded in the range of 400-1000 cm^{-1} (see Fig.1) exhibit two absorption bands below 600 cm^{-1} which is attributed to metal oxygen (M–O) vibrational modes [26]. The high frequency band observed in the frequency range 521-535 cm^{-1} is attributed to the presence of metal ions at the tetrahedral sites [27], which reflects the local lattice effect in the tetrahedral sub-lattice. The low frequency band located at about 404-412 cm^{-1} corresponds to the characteristics of the octahedral bonds [28], showing the local lattice effect in the octahedral sub-lattice. The bands observed at 521-535 cm^{-1} and 404-412 cm^{-1} (Table I) confirm the presence of Fe^{3+} ions on both tetrahedral and octahedral sites, respectively [29].

3.2. Structural Analysis

The XRD patterns of $\text{Zn}_{1-x}\text{Co}_x\text{Gd}_y\text{Fe}_{2-y}\text{O}_4$ ($x=0.0-0.5$, $y=0.00-0.10$) ferrites are shown in Fig. 2. It can be seen that all the samples exhibit cubic spinel structure as a major phase and GdFeO_3 as a secondary phase (denoted by asterisk in the XRD patterns) [30]. The lattice constant ‘a’ for the un-substituted ferrite sample is larger than the substituted one [31]. The secondary phase on the grain boundaries may be attributed to the high reactivity of Fe^{3+} with Gd^{3+} and limited solubility of Gd^{3+} into the spinel lattice [32, 33]. It has already been reported that Gd^{3+} solubility limit is reached at $y = 0.02$ and after the solubility limit, Gd^{3+} does not dissolve into the spinel lattice [34]. Gd^{3+} segregate on the grain boundaries instead of occupying the tetrahedral and the octahedral sites as reflected in the XRD results [33, 35]. With further increase in the Gd^{3+} content, the aggregates at grain boundaries increase resulting in the further compression of the spinel lattice [36, 37]. It has already been reported that lattice parameter decreases with the addition of Gd^{3+}

which can be attributed to the solubility limit at $y=0.02$ and aggregates at the grain boundaries [34]. The decrease in the lattice constant is due to the replacement of Zn^{2+} with Co^{2+} since ionic size of Co^{2+} (0.78 Å) is smaller than that of Zn^{2+} (0.82 Å) which has been reported earlier [38]. The values of the lattice constant lie in the range of 8.415-8.480 Å (Table I) that are in good agreement with the previously reported values [36]. The values of unit cell volume of the samples are listed in Table I.

3.3. Scanning Electron Microscopy (SEM) Analysis:

Scanning electron microscopy was used to examine the morphology and grain size of the investigated samples. Figure 3 shows the SEM profiles of a few representative samples. It is evident from the micrographs that the materials are fine grained and the particle sizes are uniformly distributed. Few agglomerates can be observed, which may be the result of the high sintering temperature. Grain size of these samples was also estimated by using the line intercept method [39]. The average grain size decreases in the range of 0.76 to 0.18 μm depending upon the substituted amount of cations (Table I). It is also obvious from these micrographs that as Gd content increased in the spinel lattice, the grain size became smaller for the substituted samples [30, 31, 40]. This may be attributed to the mobility of the grain boundaries, as the close proximity of the Gd ions potentially hinder grain boundary movement. Consequently, the grain size decreases with an increasing concentration of Gd [32, 37, 41]. The Gd-substituted samples show dark ferrite matrix grains and whitish grains due to biphasic microstructure (the second phase) already reported [30, 42, 43]. Whitish grains confirm the presence of Gadolinium at grain boundaries forming $GdFeO_3$ [43].

3.4. Quantitative analysis (EDX)

The energy dispersive X-ray (EDX) spectra of few representative samples are shown in Fig. 4. The analysis of the spectra confirmed the presence of the constituent elements in the synthesized samples. Quantitative estimation of proportions of elements present in these materials are listed in Table II.

3.5. Magnetic properties

Figure 5 shows the M-H loops of $\text{Zn}_{1-x}\text{Co}_x\text{Gd}_y\text{Fe}_{2-y}\text{O}_4$ ($x=0.0-0.5$, $y=0.00$ to 0.10) ferrites with the maximum magnetic applied field being 18 kOe. Both saturation magnetization and remanence increases from 4.2 to 21.0 emu/g and 0.009 to 7.0 emu/g respectively with increasing Co-Gd contents, which is in agreement with previously reported results [44]. The saturation magnetization increases due to strong AB-interactions. The reason for increase of both saturation magnetization and coercivity is due to replacement of Zn^{2+} with Co^{2+} . As Zn^{2+} ions are replaced with Co^{2+} ions in the lattice, the saturation magnetization and the coercivity increase due to the anisotropic nature of Co^{2+} as previously reported [9]. It has been reported earlier that small amount of rare-earth ions incorporated in the ferrite favor the formation of the secondary phases associated with modifications in the magnetic properties [45]. The increase in coercivity with increase in Gd content has already been reported in the Gd substituted ferrites [30]. With increase in the substitution of Gadolinium, the surplus Gd^{3+} ions form a secondary phase at grain boundaries. This is due to Gd ions being too large to occupy the tetrahedral or octahedral sites during sintering process and secondary phase is formed [31]. The secondary phase may affect the homogenous composition and microstructure, and also induces distortion within the grains that may lead to a larger internal stress [30]. Such a stress hinders the growth of grains. In our study, with increase in Gd content, grain boundaries increase with decrease in grain size [31]. The area of disordered arrangement of atoms at grain boundaries may hinder the domain wall motion, thus coercivity of samples increases with increasing Gd content [30, 31]. Azhar et al. [46] has also reported that the increase in coercivity is related with the appearance of second phase which impedes the domain wall motion. Roy et al. [47] reported that coercivity is inversely proportional to grain size: when grain size decreases, coercivity increases [47, 48]. Saturation magnetization increases with increase in Gd-content and decrease in grain size as reported earlier [30]. Presence of Gd^{3+} ions at the grain boundaries would exert a pressure on the grains, which might increase the magnitude of the magnetic interactions and cause increase in magnetization as reported earlier [31]. Here the pressure at the grain boundaries is the main reason for the increasing magnetization [31]. Figure 5 reveals an increasing trend of coercive field with increasing CoGd contents [37]. It has been observed that the coercivity increases in the range 21.7-869.6 Oe [9]. The factors that influence the coercivity include morphology, magnetocrystalline anisotropy, the domain sizes, etc. [49]. The squareness ratio (M_r/M_s) lies in the range 0.00-0.33, well below the typical value 1 [50]. In the present case, it has been assumed that the particles are single domain.

3.6. MCP

Figure 6 shows the frequency dependent complex permittivity (ϵ_{eff}' and ϵ_{eff}'') spectra of $\text{Zn}_{1-x}\text{Co}_x\text{Gd}_y\text{Fe}_{2-y}\text{O}_4$ ($x=0.0-0.5$, $y=0.00$ to 0.10) ferrites in the frequency range 2.5 to 6.8 GHz. The real part of complex permittivity shows very little frequency dependence and is almost constant [51] while the imaginary part, decreasing at first, becomes almost constant at high frequencies [36]. Permittivity values have been found to be quite low in the microwave region [52]. At high frequencies, permittivity of ferrite materials mainly depends on the atomic and electronic polarization within the grains [11, 53]. The relaxation of these mechanisms are much higher at microwave frequencies, and thus the frequency dependent contribution to ϵ' is minimal and ϵ'' is a result of other loss mechanisms such as defects and porosity present in the samples. Figure 7 shows the frequency dependent complex permeability spectra of $\text{Zn}_{1-x}\text{Co}_x\text{Gd}_y\text{Fe}_{2-y}\text{O}_4$ ($x=0.0-0.5$, $y=0.00$ to 0.10) ferrites in the frequency range 3.8 to 10.16 GHz. It was earlier reported that to design a high quality absorber a large value of permeability of absorption material should be obtained [45-50] and by doping Co, large complex permeability can be obtained [54]. It is obvious that complex permeability (both real and imaginary parts) of $\text{Zn}_{1-x}\text{Co}_x\text{Gd}_y\text{Fe}_{2-y}\text{O}_4$ ($x=0.0-0.5$, $y=0.00$ to 0.10) ferrites increases with the increase in CoGd content [46] and decreases with increasing frequency [55]. The decreasing behavior of complex permeability can be explained by the relaxation phenomenon of domain wall motion and rotation in the GHz region with the increase of frequency [55, 56].

Conclusions

The CoGd co-substituted ferrites were successfully synthesized by co-precipitation technique. The synthesized ferrites exhibit cubic spinel structure with appearance of a secondary GdFeO_3 phase. FTIR Spectra and XRD confirmed the Spinel phase formation. The lattice constant decreases due to the solubility limit of Gd in the spinel lattice with increase in CoGd content. SEM images shows decrease in grain size from 0.76 to 0.18 μm with increase of CoGd content. EXD spectra reveals the presence of all the constituent metal ions in the synthesized ferrites. The saturation magnetization increases with increase of CoGd contents due to the strengthening of AB-interactions. Coercivity of un-substituted zinc ferrites is small but It increases with increasing CoGd co-substituted contents due to rise of magnetic anisotropy. Based on the ability to tune the

magnetic and microwave properties of $Zn_{1-x}Co_xGd_yFe_{2-y}O_4$, these ferrites may be a good potential candidate for an electromagnetic absorber.

Acknowledgements

The authors are thankful to the Higher Education Commission (HEC) of Pakistan for the financial assistance provided under the HEC International Research Support Initiative Program (IRSIP).

References

- [1] A.V. Ramona Reddy, G. Ranga Mohan, D. Revinder, B.S. Boyanov, “High-frequency dielectric behaviour of polycrystalline zinc substituted cobalt ferrites” *J. Mater. Sci.* 34 (1999) 3169.
- [2] J. Kulikowski, “Soft magnetic ferrites-development or stagnation?” *J. Magn. Magn. Mater.* 41 (1984) 56.
- [3] A. Goldman, “Modern Ferrite Technology” 2nd Ed., Springer, New York(2006).
- [4] Y. Köseoglu, A. Baykal, F. Gözüak, “Structural and magnetic properties of $\text{Co}_x\text{Zn}_{1-x}\text{Fe}_2\text{O}_4$ nanocrystals synthesized by microwave method” *Polyhedron* 28 (2009) 2887–2892.
- [5] R. N. Bhowmik and R. Ranganathan, “Magnetic properties in rare-earth substituted spinel $\text{Co}_{0.2}\text{Zn}_{0.8}\text{Fe}_{2-x}\text{RE}_x\text{O}_4$ (RE= Dy, Ho and Er, $x= 0.05$)” *J. Alloy. Compd.* 326 (2001) 128-131.
- [6] N. Sharma, P. Aghamkar, S. Kumar, M. Bansal, Anju , R.P.Tondon, “Study of structural and magnetic properties of Nd doped zinc ferrites” *J. Magn. Magn. Mater.* 369 (2014) 162–167.
- [7] S.G. Algude, S.M. Patange, S.E. Shirsath, D.R. Mane, K.M. Jadhav, “Elastic behaviour of Cr^{3+} substituted Co–Zn ferrites” *J. Magn. Magn. Mater.* 350 (2014) 39-41.
- [8] S. Amiri, H. Shokrollahi, “Magnetic and structural properties of RE doped Co-ferrite (RE=Nd, Eu, and Gd) nano-particles synthesized by co-precipitation” *J. Magn. Magn. Mater.* 345 (2013) 18-23.
- [9] X. Huang, J. Zhang, M. Lai, T. Sang, “Preparation and microwave absorption mechanisms of the NiZn ferrite nanofibers” *J. Alloy. Compd.* 627 (2015) 367-373.
- [10] Y. Liu, S. Wei, B. Xu, Y. Wang, H. Tian, H. Tong, “Effect of heat treatment on microwave absorption properties of Ni–Zn–Mg–La ferrite nanoparticles” *J. Magn. Magn. Mater.* 349 (2014) 57–62.
- [11] J.-L. Xie, M. Han, L. Chen, R. Kuang, L. Deng, “Microwave-absorbing properties of NiCoZn spinel ferrites” *J. Magn. Magn. Mater.* 314 (2007) 37-42.

- [12] M.C. Dimri, S. C. Kashyap, D.C. Dube, S.K. Mohanta, "Complex permittivity and permeability of Co-substituted NiCuZn ferrite at rf and microwave frequencies" *J. Electroceram.* 16 (2006)331-335.
- [13] S.T. Mahmud, A.K.M. Akther Hossain, A.K.M. Abdul Hakim, M. Seki, T. Kawai, H. Tabata, "Influence of microstructure on the complex permeability of spinel type Ni–Zn ferrite" *J. Magn. Magn. Mater.* 305 (2006) 269-274.
- [14] D.R. Cornejo, A.Medina-Boudri, J. Matutes-Aquino, "Time-dependent magnetization in co-precipitated cobalt ferrite" *Physica B* 320 (2002) 270-273.
- [15] X. Yi, Q. Yitaia, L. Jinga, Y. Li, "Hydrothermal preparation and characterization of ultrafine powders of ferrite spinels MFe_2O_4 (M= Fe, Zn and Ni)" *Materials Science and Engineering B* 34 (1995) L1-L3.
- [16] K.C.Patil, S.T. Aruna, T. Mimani, "Combustion synthesis: an update" *Current Opinion in Solid State and Materials Science* 6 (2002) 507-512.
- [17] V. Pillai, D.O. Shah, "Synthesis of high-coercivity cobalt ferrite particles using water-in-oil microemulsions" *J. Magn. Magn. Mater.* 163 (1996) 243-248.
- [18] X.-M. Liu, S.-Y. Fu, H.-M. Xiao, C.-J.Huang, "Synthesis of nanocrystalline spinel $CoFe_2O_4$ via a polymer-pyrolysis route" *Physica B:Condensed Matter* 370 (2005) 14-21.
- [19] W.C. Kim, S.W. Lee, S.J. Kim, S.H. Yoon, C.S. Kim, "Magnetic properties of Y-, La-, Nd-, Gd-, and Bi-doped ultrafine $CoFe_2O_4$ spinel grown by using a sol–gel method" *J. Magn. Magn. Mater.* 215-216 (2000) 217-220.
- [20] E. Pervaiz, I.H. Gul, "Influence of rare earth (Gd^{3+}) on structural, gigahertz dielectric and magnetic studies of cobalt ferrite" *Journal of Physics: Conference Series*, 439 (2013) 012015.
- [21] Q. Lin, J. Lin, Y. He, R. Wang, J. Dong, "The Structural and Magnetic Properties of Gadolinium Doped $CoFe_2O_4$ Nanoferrites" *Journal of Nanomaterials*, 2015, 294239.
- [22] M.T. Rehman, M. Vargas, C.V. Raman, "Structural characteristics, electrical conduction and dielectric properties of gadolinium substituted cobalt ferrite" *Journal of Alloys and Compounds* 617 (2014) 547-562.
- [23] J.A. Cuenca, K. Bugler, S. Taylor, D. Morgan, P. Williams, J. Bauer, A. Porch, "Study of the magnetite to maghemite transition using microwave permittivity and permeability measurements" *J. Condens. Matter Phys.* 28 (2016) 106002.

- [24] J.A. Cuenca, E. Thomas, S. Mandal, O. Williams, A. Porch, "Investigating the Broadband Microwave Absorption of Nanodiamond Impurities" *IEEE Transactions on Microwave Theory and Techniques* 63 (2015) 4110-4118.
- [25] J.A. Cuenca, E. Thomas, S.Mandal, O.Williams, A. Porch, "Microwave determination of sp² carbon fraction in nanodiamond powders" *Carbon* 81 (2015) 174-178.
- [26] A.M. El-Sayed, "Effect of chromium substitutions on some properties of NiZn ferrites" *Ceram Int.* 28 (2002) 651-655.
- [27] L.J. Berchmans, R.K. Selvan, P.N.S. Kumar, C.O. Augustin, "Structural and electrical properties of Ni_{1-x}Mg_xFe₂O₄ synthesized by citrate gel process" *J. Magn. Magn. Mater.* 279 (2004) 103-110.
- [28] S.C. Watawe, B.D. Sutar, B.D. Sarwade, B.K. Chougule, "Infrared studies of some mixed Li-Co ferrites" *International Journal of Inorganic Materials* 3 (2001) 819-823.
- [29] M.A Ahmed, E Ateia, S.I. El-Dek, "Spectroscopic analysis of ferrite doped with different rare earth elements" *J. Vibrational Spectroscopy* 30 (2002) 69-75.
- [30] Nilar Lwin, Ahmad Fauzi M.N., Srimal Sreekantan, Radzali Othman, "Physical and electromagnetic properties of nanosized Gd substituted Mg-Mn ferrites by solution combustion method" *Physica B* 461 (2015) 134-139.
- [31] Lijun Zhao, Hua Yang, Lianxiang Yu, Wei Sun, Yuming Cui, Yu Yan, Shouhua Feng, "Structure and magnetic properties of Ni_{0.7}Mn_{0.3}Fe₂O₄ nanoparticles doped with La₂O₃" *Phys. Stat. Sol. (a)* 201 (2014) 3121-3128.
- [32] Ishtiaq Ahmad, Mahmood Ahmad, Ihsan Ali, M. Kanwal, M.S. Awan, Ghulam Mustafa, and Mukhtar Ahmad, "Effects of Gd-Substitutions on the Microstructure, Electrical and Electromagnetic Behavior of M-Type Hexagonal Ferrites" *J. Electron. Mater.* 44 (2015) 2221-2229.
- [33] Lijun Zhao, Yuming Cui, Hua Yang, Lianxiang Yu, Weique Jin, Shouhua Feng, "The magnetic properties of Ni_{0.7}Mn_{0.3}Gd_xFe_{2-x}O₄ ferrite" *Materials Letters* 60 (2006) 104-108.
- [34] Ahmed Abo Arais, "Gd³⁺ ions doping effect on the microstructure and electrical properties of Mn_{0.9}Zn_{0.1}Ni_{0.05}Ti_{0.05}Gd_tFe_{1.9-t}O₄ ferrite" *International Journal of Scientific & Engineering Research* 7 (2016) 1797-1809.
- [35] M.A Ahmed, E Ateia, S.I El-Dek, "Rare earth doping effect on the structural and electrical properties of Mg-Ti ferrite" *Materials Letters* 57 (2003) 4256-4266.

- [36] M. Asif Iqbal, Misbah-ul-Islam, Irshad Ali, Hassan M. Khan, Ghulam Mustafa, Ihsan Ali, "Study of electrical transport properties of Eu^{+3} substituted MnZn-ferrites synthesized by co-precipitation technique" *Ceramic International* 39 (2013) 1539-1545.
- [37] M. Asif Iqbal, Misbah-ul Islam, Muhammad Naeem Ashiq, Irshad Ali, Aisha Iftikhar, Hasan M. Khan, "Effect of Gd-substitution on physical and magnetic properties of $\text{Li}_{1.2}\text{Mg}_{0.4}\text{Gd}_x\text{Fe}_{2-x}\text{O}_4$ ferrites" *J. Alloy. Compd.* 579 (2013) 181-186.
- [38] S. Nasrin, S. Manjura Hoque, F.-U.-Z Chowdhury, M. Moazzam Hossen, "Influence of Zn substitution on the structural and magnetic properties of $\text{Co}_{1-x}\text{Zn}_x\text{Fe}_2\text{O}_4$ nano-ferrites" *IOSR Journal of Applied Physics* 6 (2), Ver. III (2014) 58-65.
- [39] Mukhtar Ahmad, R. Grössinger, M. Kriegisch, F. Kubel, M.U. Rana, "Magnetic and microwave attenuation behavior of Al-substituted Co₂W hexaferrites synthesized by sol-gel autocombustion process" *Current Applied Physics* 12 (2012) 1413-1420.
- [40] T. J. Shinde. A. B. Gadkari, P. N. Vasambekar, "Saturation magnetization and structural analysis of $\text{Ni}_{0.6}\text{Zn}_{0.4}\text{Nd}_y\text{Fe}_{2-y}\text{O}_4$ by XRD, IR and SEM techniques" *J. Mater. Sci.: Mater Electron* 21 (2010) 120-124.
- [41] Mukhtar Ahmad, Faiza Aen, M.U. Islam, Shahida B. Niazi, M.U. Rana, "Structural, physical, magnetic and electrical properties of La-substituted W-type hexagonal ferrites" *Ceramic International* 37 (2011) 3691-3696.
- [42] K. Muthuraman, S. Alagarsamy, M. Ameena Banu, Vasant Naidu, "Synthesis of Nano sized Ce-Co Doped Zinc Ferrite and their Permittivity and Hysteresis Studies" *International Journal of Computer Applications* 32 (2011) 18-27.
- [43] P.K. Roy, J. Bera, "Electromagnetic properties of samarium-substituted NiCuZn ferrite prepared by auto-combustion method" *Journal of Magnetism and Magnetic Materials* 321 (2009) 247-251.
- [44] M.M. Eltabey, W.R. Agami, H.T. Mohsen, Bera, "Improvement of the magnetic properties for Mn-Ni-Zn ferrites by rare earth Nd^{3+} ion substitution" *Journal of Advanced Research* 5 (2014) 601-605.
- [45] M.A. Ahmed, N. Okasha, M.M. El-Sayed, "Enhancement of the physical properties of rare-earth-substituted Mn-Zn ferrites prepared by flash method" *Ceramics International* 33 (2007) 49-58.

- [46] M. Azhar Khan , M.U. Islam, M. Ishaque, I.Z. Rahman, “Effect of Tb substitution on structural, magnetic and electrical properties of magnesium ferrites” *Ceramics International* 37 (2011) 2519-2526.
- [47] P.K. Roy, Bibhuti B. Nayak, J. Bera, “Study on electro-magnetic properties of La substituted Ni-Cu-Zn ferrite synthesized by auto-combustion method” *Journal of Magnetism and Magnetic Materials* 320 (2008) 1128-1132.
- [48] Razia Nongjai, Shakeel Khan, K. Asokan, Hilal Ahmed, and Imran Khan, “Magnetic and electrical properties of In doped cobalt ferrite nanoparticles”, *Journal of Applied Physics* 112 (2012) 084321.
- [49] Ghulam Mustafa, M.U. Islam, Wanli Zhang, Yasir Jamil, M. Asif Iqbal, Mudassar Hussain, Mukhtar Ahmad, “Temperature dependent structural and magnetic properties of Cerium substituted Co-Cr ferrite prepared by auto-combustion method” *J. Magn. Magn. Mater.* 378 (2015) 409-416.
- [50] Daliya S.Mathew, Ruey Shin Juang, “An overview of the structure and magnetism of spinel ferrite nanoparticles and their synthesis in microemulsions” *J. Chemical Eng.* 129 (2007) 51-65.
- [51] M. Ishaque, Muhammad Azhar Khan, Irshad Ali, Hasan M.Khan, M. Asif Iqbal, M.U. Islam, Muhammad Farooq Warsi, “Investigations on structural, electrical and dielectric properties of yttrium substituted Mg-ferrites” *Ceram. Int.* 41 (2015) 4028-4034.
- [52] A. Globus, “I.- Magnetization mechanisms some physical considerations about the domain wall size theory of magnetization mechanisms *J. Phys. Colloques* 38 (1977) C1-1-C1-15.
- [53] Mukhtar Ahmad, Ihsan Ali, R. Grössinger, M. Kriegisch, F. Kubel, M.U. Rana, “Effects of divalent ions substitution on the microstructure, magnetic and electromagnetic parameters of Co₂W hexagonal ferrites synthesized by sol–gel method” *J. Alloy. Compd.* 579 (2013) 57-64.
- [54] Yin Guanjun, Liao Shaobin, “Complex Permeability in absorption materials of spinel ferrites” *Beijing Daxue Xuebao*, Vol. 26, Nr. 3, 1990, pp 327-332.
- [55] Adriana Medeiros Gama, Mirabel Cerqueira Rezende, “Complex permeability and permittivity variation of radar absorbing materials based on MnZn ferrite in microwave frequencies” *Materials Research* 16 (2013) 997-1001.

- [56] R.S. Meena, S. Bhattacharya, R. Chatterjee, "Complex permittivity, permeability and microwave absorbing studies of $(\text{Co}_{2-x}\text{Mn}_x)$ U-type hexaferrite for X-band (8.2-12.4 GHz) frequencies" *Mater. Sci. Eng. B: Solid State Adv. Technol.* 171 (2010) 133-138.

Figure Captions

- Figure 1.** FTIR spectra of $Zn_{1-x}Co_xGd_yFe_{2-y}O_4$ ferrites ($x=0.1-0.5$, $y=0.02-0.10$)
- Figure 2.** XRD patterns of $Zn_{1-x}Co_xGd_yFe_{2-y}O_4$ ferrites ($x=0.0-0.5$, $y=0.00-0.10$)
- Figure 3.** SEM micrographs of $Zn_{1-x}Co_xGd_yFe_{2-y}O_4$ ferrites ($x=0.1$, $y=0.02$), ($x=0.2$, $y=0.04$), ($x=0.3$, $y=0.06$) and ($x=0.5$, $y=0.10$)
- Figure 4.** EDX spectrum of $Zn_{1-x}Co_xGd_yFe_{2-y}O_4$ ferrites ($x=0.2$, $y=0.04$) and ($x=0.4$, $y=0.08$)
- Figure 5.** M-H Loops of co-substituted $Zn_{1-x}Co_xGd_yFe_{2-y}O_4$ ferrites ($x=0.0-0.5$, $y=0.00-0.10$)
- Figure 6.** (a) Real and (b) imaginary parts of effective complex permittivity of co-substituted $Zn_{1-x}Co_xGd_yFe_{2-y}O_4$ ferrites ($x=0.0-0.5$, $y=0.00-0.10$)
- Figure 7.** (a) Real and (b) imaginary parts of effective complex permeability of co-substituted $Zn_{1-x}Co_xGd_yFe_{2-y}O_4$ ferrites ($x=0.0-0.5$, $y=0.00-0.10$)

Table Captions

Table I. High frequency band (ν_1), Low frequency band (ν_2), Lattice constant (a), Unit cell volume (V) and Grain size of $Zn_{1-x}Co_xGd_yFe_{2-y}O_4$ ferrites ($x=0.0-0.5$, $y=0.00-0.10$)

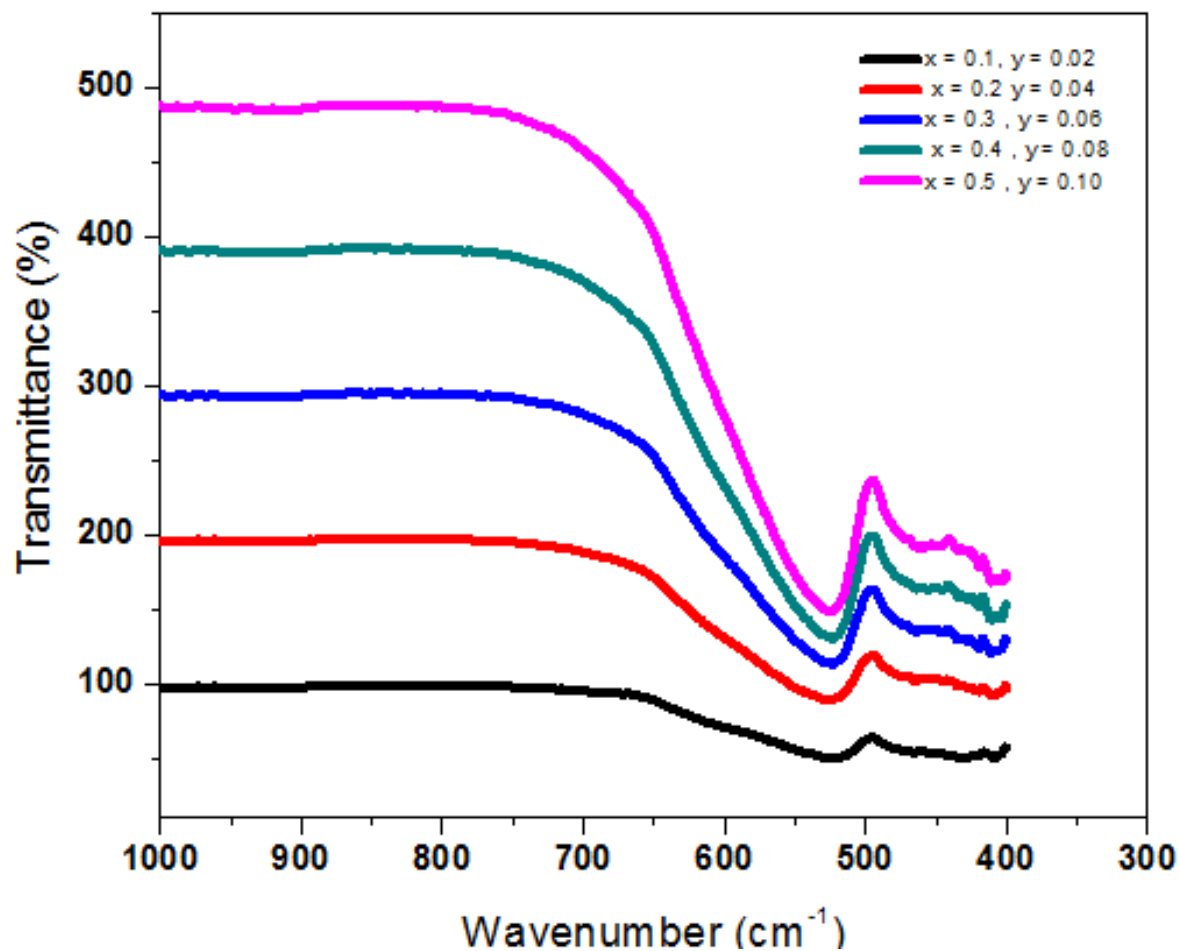
Table II. Quantitative estimation of elements (weight %) for $Zn_{1-x}Co_xGd_yFe_{2-y}O_4$ ferrites ($x=0.0-0.5$, $y=0.00-0.10$) obtained from EDX analysis

Table III. Saturation Magnetization (Ms), Remanence (Mr), Coercivity (Hc), and Squareness Ratio (Mr/Ms) of $Zn_{1-x}Co_xGd_yFe_{2-y}O_4$ ferrites ($x=0.0-0.5$, $y=0.00-0.10$)

Title: Microwave Absorption Properties of CoGd Substituted ZnFe₂O₄ ...

Author: M. Hussain, Misbah-ul-Islam, T. Meydan, *et al.*

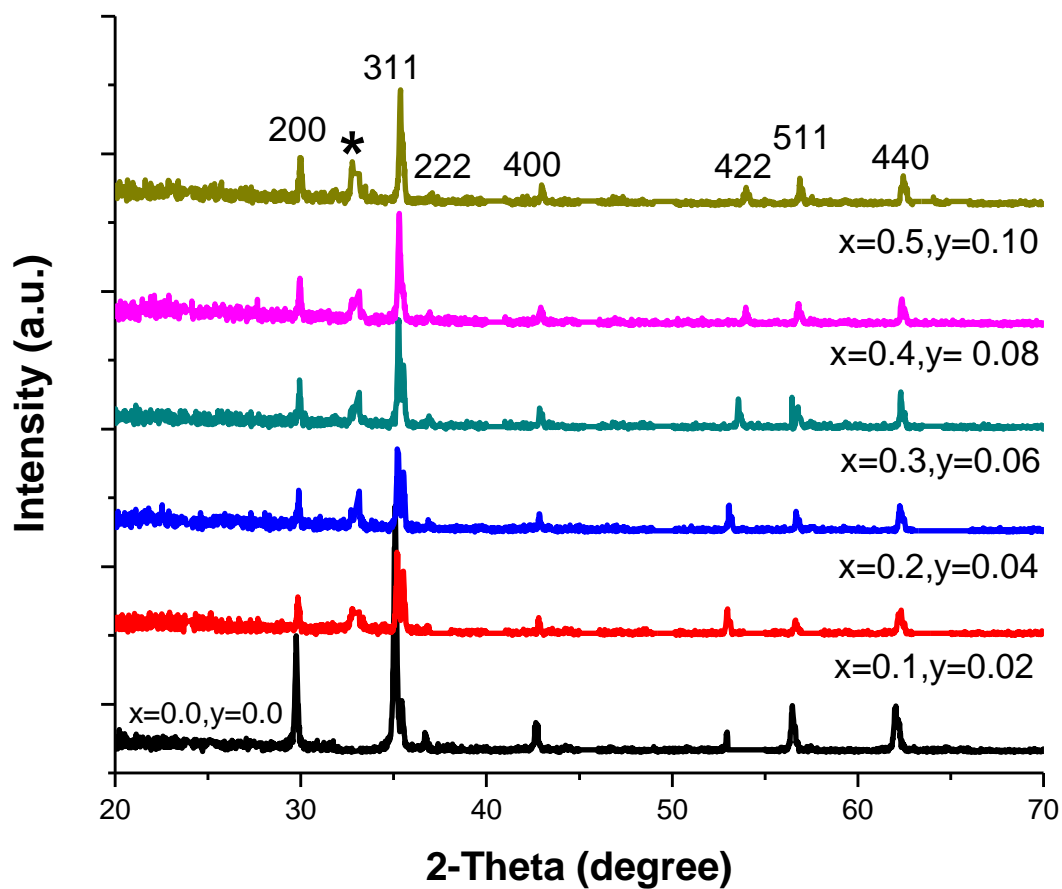
Figure 1. FTIR spectra of Zn_{1-x}Co_xGd_yFe_{2-y}O₄ ferrites (x=0.1-0.5, y=0.02-0.10)



Title: Microwave Absorption Properties of CoGd Substituted ZnFe₂O₄ ...

Author: M. Hussain, Misbah-ul-Islam, T. Meydan, *et al.*

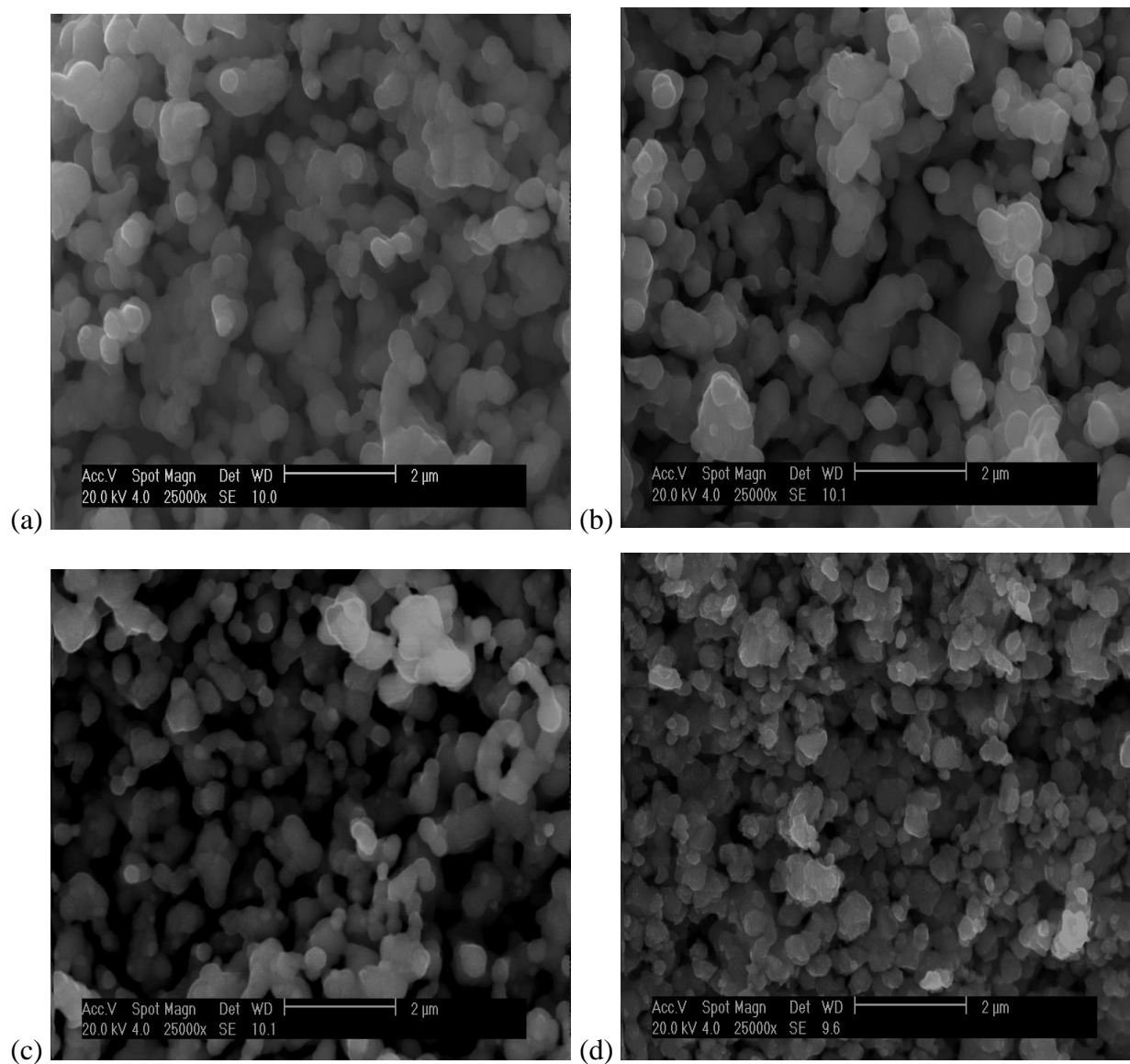
Figure 2. XRD patterns of Zn_{1-x}Co_xGd_yFe_{2-y}O₄ ferrites (x=0.0-0.5, y=0.00-0.10)



Title: Microwave Absorption Properties of CoGd Substituted ZnFe_2O_4 ...

Author: M. Hussain, Misbah-ul-Islam, T. Meydan, *et al.*

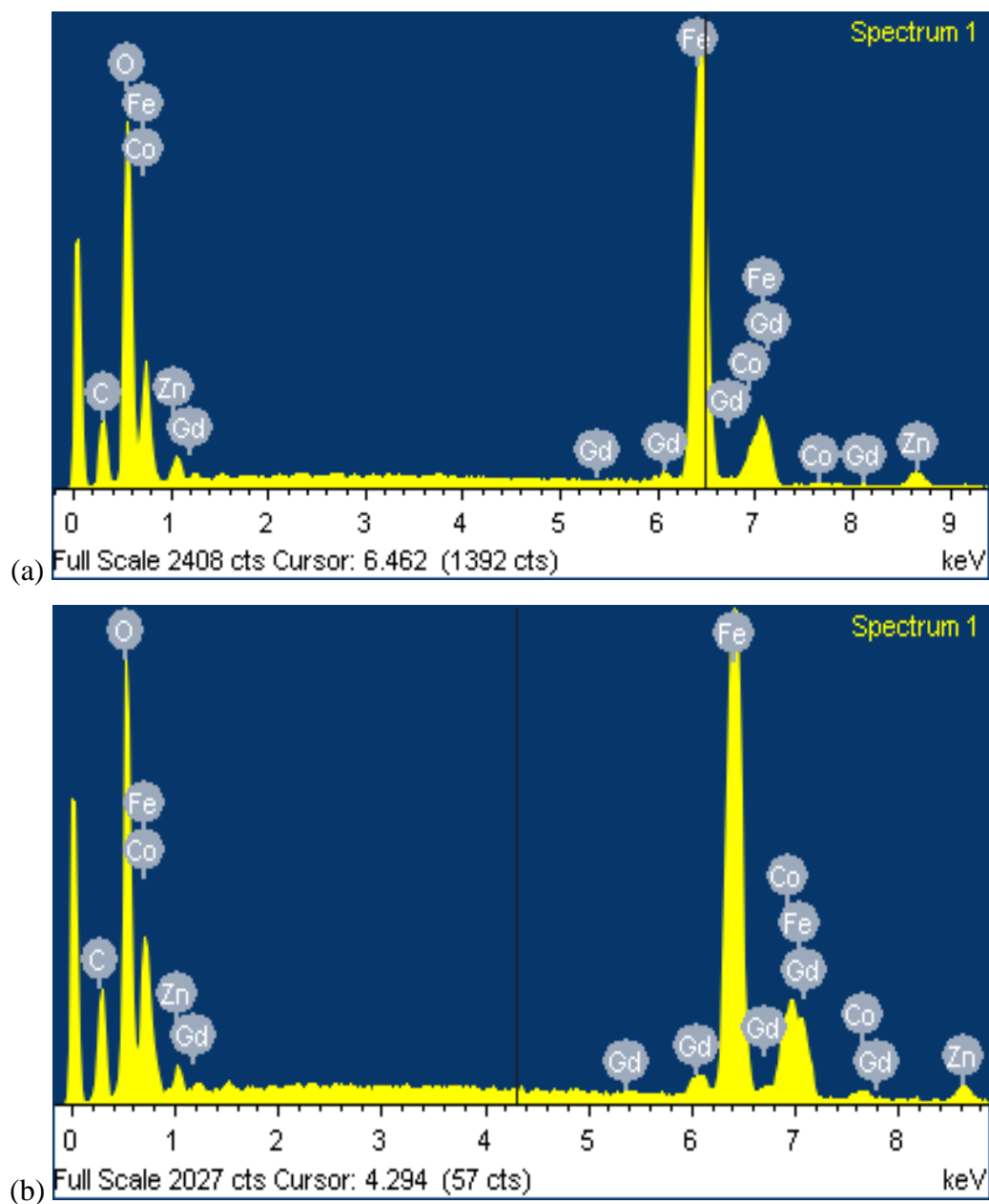
Figure 3. SEM micrographs of $\text{Zn}_{1-x}\text{Co}_x\text{Gd}_y\text{Fe}_{2-y}\text{O}_4$ ferrites for (a) $x=0.1, y=0.02$, (b) $x=0.2, y=0.04$, (c) $x=0.3, y=0.06$ and (d) $x=0.5, y=0.10$



Title: Microwave Absorption Properties of CoGd Substituted ZnFe₂O₄ ...

Author: M. Hussain, Misbah-ul-Islam, T. Meydan, *et al.*

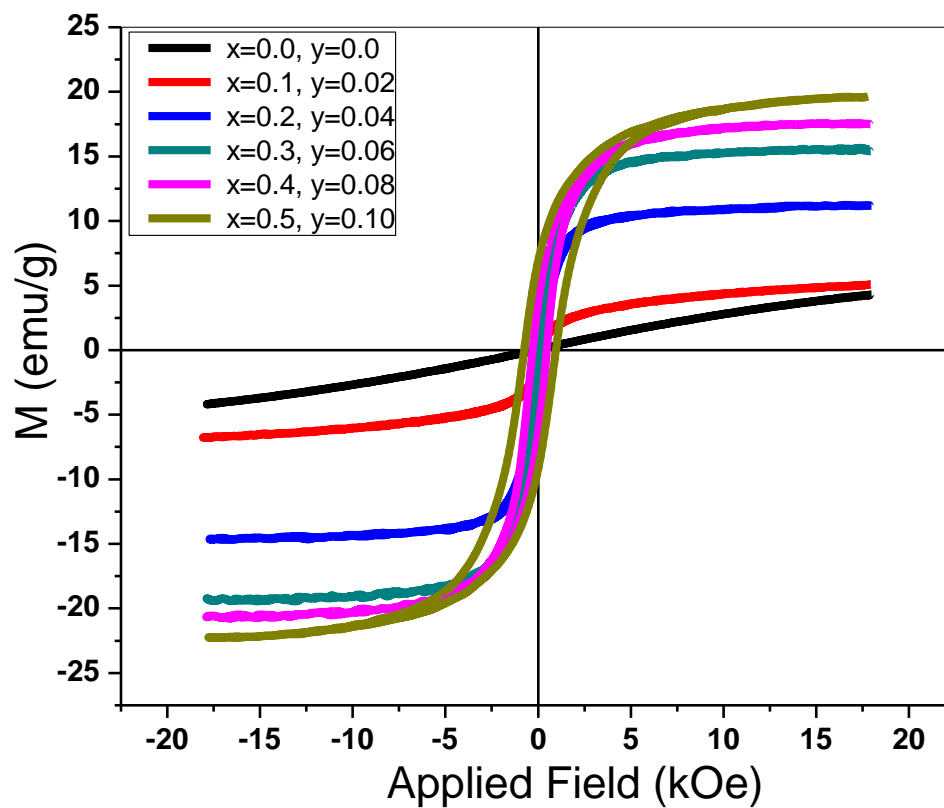
Figure 4. EDX spectrum of Zn_{1-x}Co_xGd_yFe_{2-y}O₄ ferrites for (a) x=0.2, y=0.04 and (b) x=0.4, y=0.08



Title: Microwave Absorption Properties of CoGd Substituted ZnFe₂O₄ ...

Author: M. Hussain, Misbah-ul-Islam, T. Meydan, *et al.*

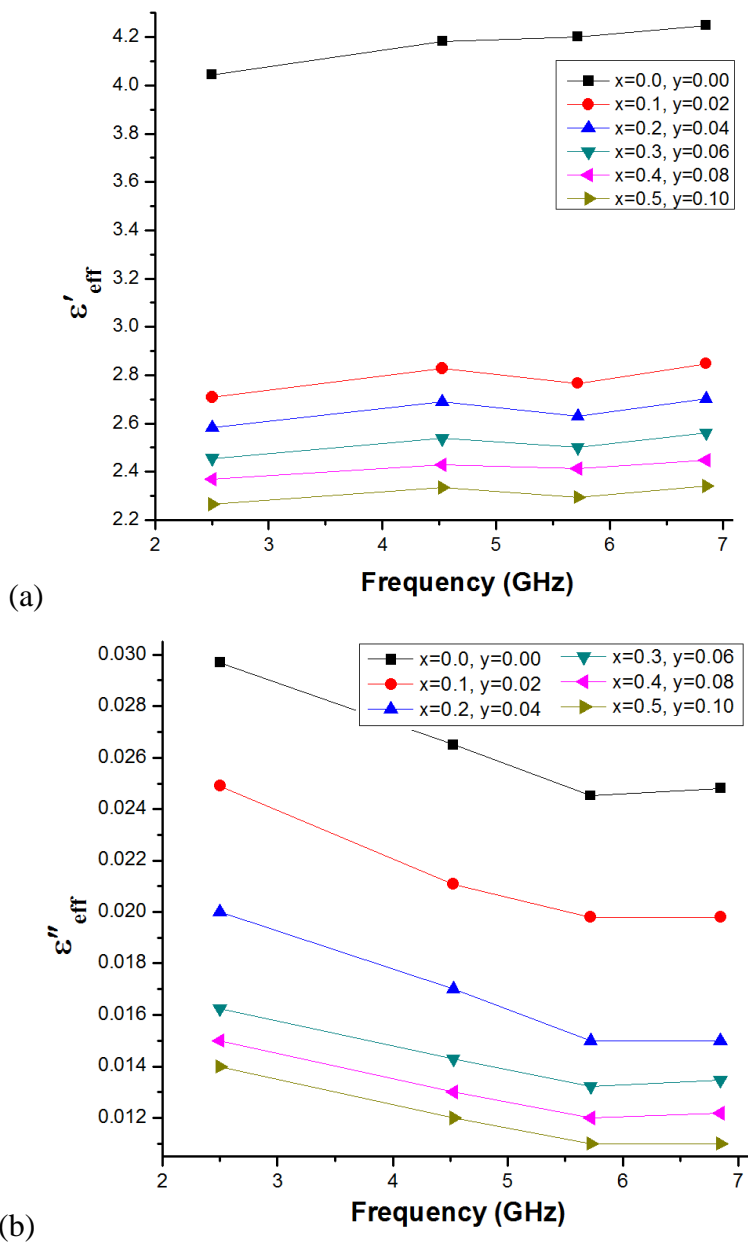
Figure 5. M-H Loops of co-substituted Zn_{1-x}Co_xGd_yFe_{2-y}O₄ ferrites (x=0.0-0.5, y=0.00-0.10)



Title: Microwave Absorption Properties of CoGd Substituted ZnFe₂O₄ ...

Author: M. Hussain, Misbah-ul-Islam, T. Meydan, *et al.*

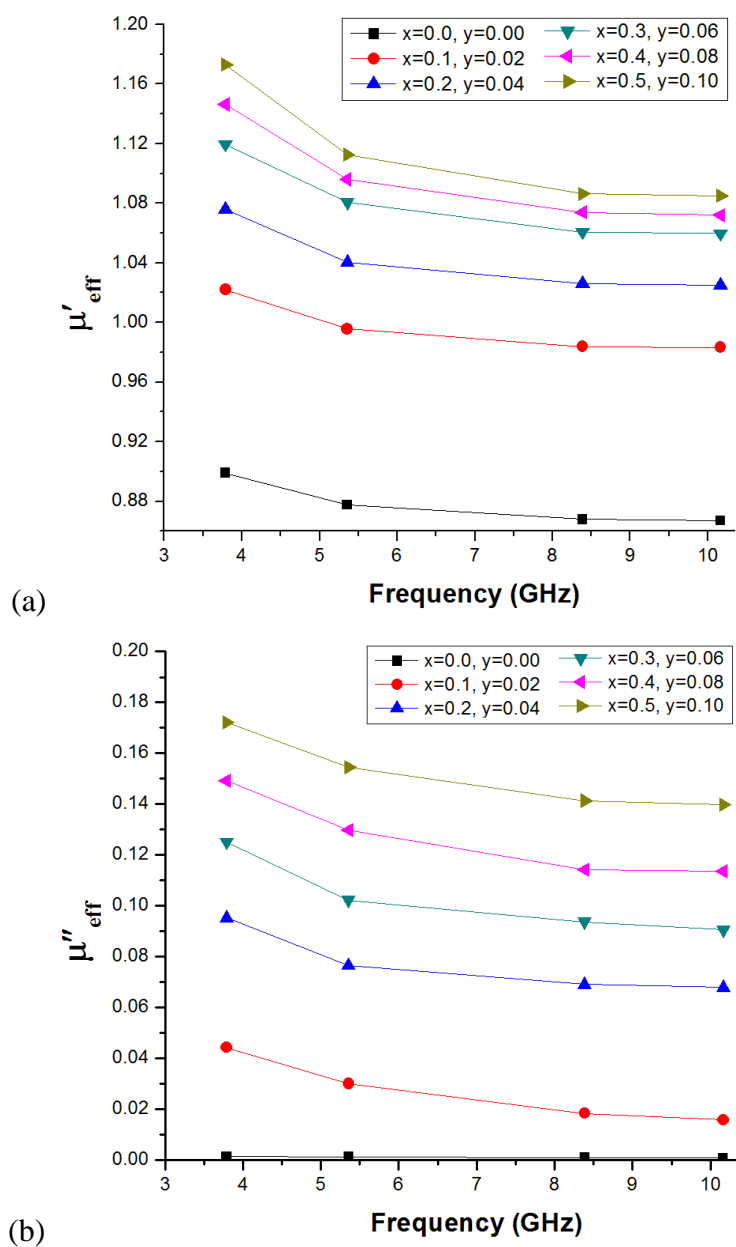
Figure 6. (a) Real and (b) imaginary parts of effective complex permittivity of co-substituted Zn_{1-x}Co_xGd_yFe_{2-y}O₄ ferrites (x=0.0-0.5, y=0.00-0.10)



Title: Microwave Absorption Properties of CoGd Substituted ZnFe_2O_4 ...

Author: M. Hussain, Misbah-ul-Islam, T. Meydan, *et al.*

Figure 7. (a) Real and (b) imaginary parts of effective complex permeability of co-substituted $\text{Zn}_{1-x}\text{Co}_x\text{Gd}_y\text{Fe}_{2-y}\text{O}_4$ ferrites ($x=0.0-0.5$, $y=0.00-0.10$)



Title: Microwave Absorption Properties of CoGd Substituted ZnFe₂O₄ ...

Author: M. Hussain, Misbah-ul-Islam, T. Meydan, *et al.*

Table I. High frequency band (ν_1), Low frequency band (ν_2), Lattice constant (a), Unit cell volume (V) and Grain size of Zn_{1-x}Co_xGd_yFe_{2-y}O₄ ferrites (x=0.0-0.5, y=0.00-0.10)

Parameters	x=0.0,	x=0.1,	x=0.2,	x=0.3,	x=0.4,	x=0.5,
	y=0.00	y=0.02	y=0.04	y=0.06	y=0.08	y=0.10
High frequency band ν_1 (cm ⁻¹)	534.4	521.2	524.4	523.7	524.1	524.4
Low frequency band ν_2 (cm ⁻¹)	404.1	408.3	408.8	409.8	411.4	411.5
Lattice constant a (Å)	8.480	8.460	8.456	8.424	8.415	8.414
Unit Cell Volume V (Å ³)	611.28	605.45	604.75	597.85	595.98	595.69
Grain size (μm)	0.76	0.55	0.39	0.38	0.29	0.18

Title: Microwave Absorption Properties of CoGd Substituted ZnFe_2O_4 ...

Author: M. Hussain, Misbah-ul-Islam, T. Meydan, *et al.*

Table II. Quantitative estimation of elements (weight %) for $\text{Zn}_{1-x}\text{Co}_x\text{Gd}_y\text{Fe}_{2-y}\text{O}_4$ ferrites
($x=0.0-0.5$, $y=0.00-0.10$) obtained from EDX analysis

Parameters	x=0.0,	x=0.1,	x=0.2,	x=0.3,	x=0.4,	x=0.5,
	y=0.00	y=0.02	y=0.04	y=0.06	y=0.08	y=0.10
Zn (weight %)	27.15	24.26	21.43	18.64	15.92	13.19
Co (weight %)	-	2.44	4.84	7.22	9.55	11.89
Gd (weight %)	-	1.31	2.57	3.86	5.12	6.35
Fe (weight %)	46.33	45.62	44.90	44.17	43.47	42.76
O (weight %)	26.52	26.37	26.26	26.11	25.94	25.81
<i>Total</i>	100	100	100	100	100	100

Title: Microwave Absorption Properties of CoGd Substituted ZnFe₂O₄ ...

Author: M. Hussain, Misbah-ul-Islam, T. Meydan, *et al.*

Table III. Saturation Magnetization (Ms), Remanence (Mr), Coercivity (Hc), and Squareness Ratio (Mr/Ms) of Zn_{1-x}Co_xGd_yFe_{2-y}O₄ ferrites (x=0.0-0.5, y=0.00-0.10)

Parameters	x=0.0,	x=0.1,	x=0.2,	x=0.3,	x=0.4,	x=0.5,
	y=0.00	y=0.02	y=0.04	y=0.06	y=0.08	y=0.10
Saturation Magnetization, Ms (emu/g)	4.20	5.80	12.80	17.20	18.80	21.0
Remanence, Mr (emu/g)	0.009	0.25	0.38	1.300	4.60	7.000
Coercivity, Hc (Oe)	21.7	47.8	133.3	159.7	435.3	869.6
Squareness Ratio, Mr/Ms	-	0.04	0.03	0.08	0.24	0.33